Modeling plasma accelerators II: Making the simulations faster

Remi Lehe

Lawrence Berkeley National Laboratory, Berkeley, California

February 7, 2023

Reminder: Full Particle-In-Cell codes solve the Maxwell equations, along with the equations of motion for plasma and beam particles

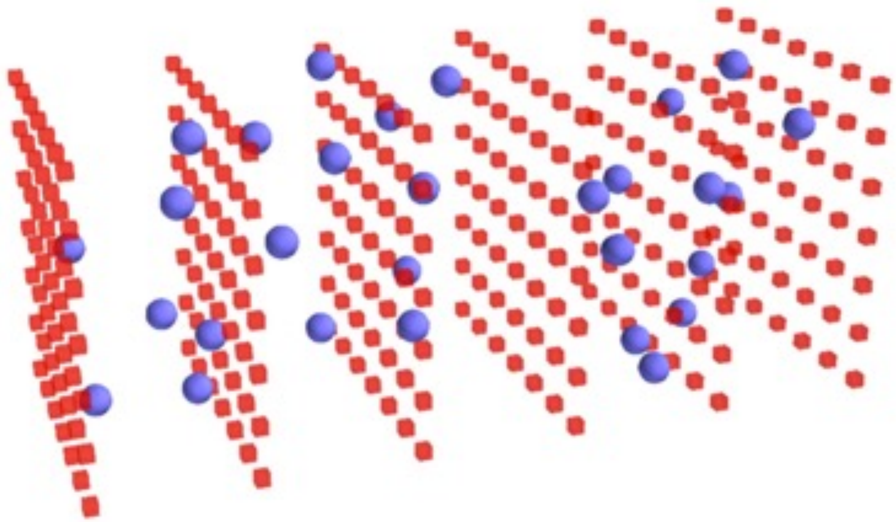

Particle push

Update $\boldsymbol{x}_i$ and $\boldsymbol{p}_i$

$$\frac{d\boldsymbol{x}_i}{dt} = \boldsymbol{v}_i$$

$$\frac{d\boldsymbol{p}_i}{dt} = q\left(\boldsymbol{E} + \boldsymbol{v}_i \times \boldsymbol{B}\right)$$

Charge/current deposition

Calculate $\rho, \boldsymbol{j}$ from the $\boldsymbol{x}_i, \boldsymbol{v}_i$

Field solver

Update $\boldsymbol{E}, \boldsymbol{B}$ using $\boldsymbol{j}$

$$\frac{\partial \boldsymbol{B}}{\partial t} = -\boldsymbol{\nabla} \times \boldsymbol{E}$$

$$\frac{\partial \boldsymbol{E}}{\partial t} = c^2 \boldsymbol{\nabla} \times \boldsymbol{B} - \mu_0 c^2 \boldsymbol{j}$$

Field gathering

Interpolate $\boldsymbol{E}, \boldsymbol{B}$ on the $\boldsymbol{x}_i$

Reminder: Full Particle-In-Cell codes can quickly become computationally expensive

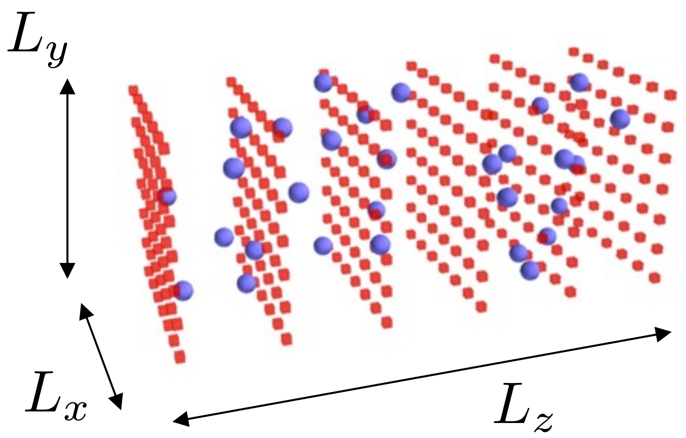

The number of computational operations scales like:

$$N_{comp} \propto \underbrace{\left(\frac{L_x}{\Delta x}\right) \times \left(\frac{L_y}{\Delta y}\right) \times \left(\frac{L_z}{\Delta z}\right)}_{\text{Number of grid points}} \times \underbrace{\left(\frac{T_{interaction}}{\Delta t}\right)}_{\text{Number of timesteps (i.e. number of iterations of the PIC loop)}}$$

$$T_{interaction} \sim \frac{L_{plasma}}{c}$$

For simulations of laser-driven acceleration:

$$\Delta z \sim \frac{\lambda}{40} \qquad \Delta t \sim \frac{\Delta z}{c} \sim \frac{\lambda}{40c}$$

Outline

- The boosted-frame technique
- Cylindrical geometry
- Laser envelope model
- Quasi-static PIC codes

Outline

- **The boosted-frame technique**
- Cylindrical geometry
- Laser envelope model
- Quasi-static PIC codes

What if we look at the situation in a different Lorentz frame?

Laboratory frame

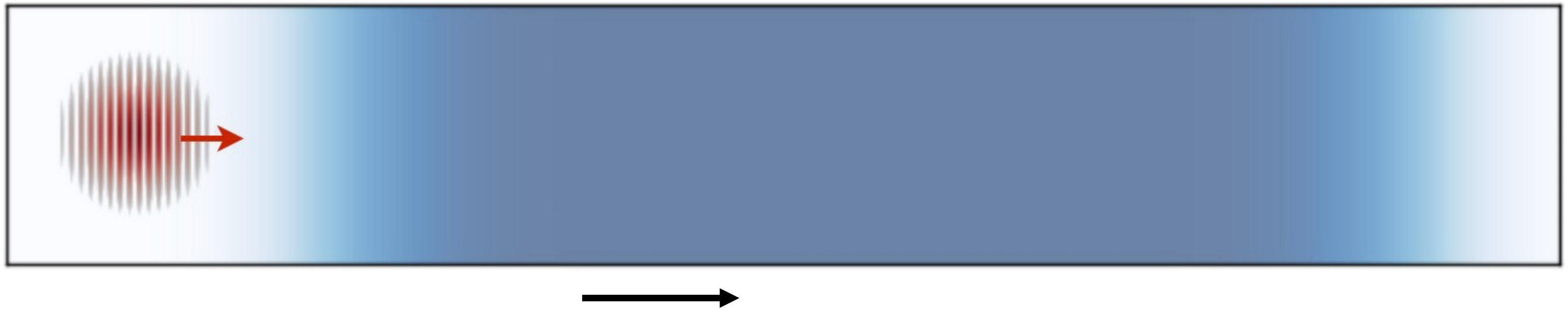

$$\beta_b = \sqrt{1 - 1/\gamma_b^2}$$

Lorentz transform,
characterized by β_b, γ_b
(typically $\gamma_b \gg 1$)

Boosted frame

The physics in the boosted frame is **equivalent**, but should **look different**.

What if we look at the situation in a different Lorentz frame?

Laboratory frame

Lorentz transform, characterized by β_b, γ_b (typically $\gamma_b \gg 1$)

$$\beta_b = \sqrt{1 - 1/\gamma_b^2}$$

Boosted frame

Dilation/contraction of length

depending on the speed of the object v_{lab}:

$$L_{boosted} = \frac{\sqrt{1-\beta_b^2}}{1-\beta_b v_{lab}/c} L_{lab}$$

- Laser pulse ($v_{lab} \approx c$):
  $L_{boosted} \approx 2\gamma_b \, L_{lab}$
- Plasma ($v_{lab} \approx 0$):
  $L_{boosted} \approx L_{lab} / \gamma_b$

What if we look at the situation in a different Lorentz frame?

Laboratory frame

$$\beta_b = \sqrt{1 - 1/\gamma_b^2}$$

Lorentz transform,
characterized by β_b, γ_b
(typically $\gamma_b \gg 1$)

- Laser pulse ($v_{lab} \approx c$):
  $L_{boosted} \approx 2\gamma_b \, L_{lab}$
- Plasma ($v_{lab} \approx 0$):
  $L_{boosted} \approx L_{lab} / \gamma_b$

Boosted frame

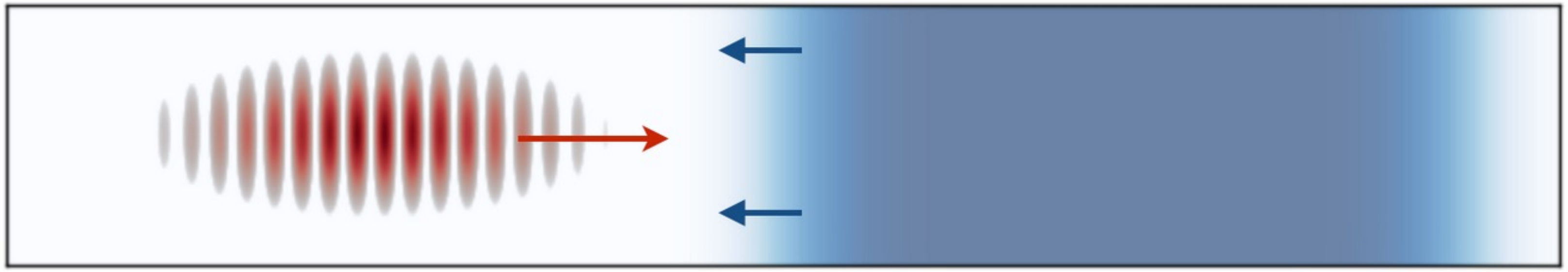

Computational advantage: simulating in the boosted frame reduces the total number of iterations.

Number of iterations needed to complete the simulation:

$$N_{iterations} = \frac{T_{interaction}}{\Delta t} \propto \frac{L_{plasma}}{\lambda}$$

The number of iterations needed is orders-of-magnitude lower in the boosted frame!

$$N_{iterations,boosted} = \frac{N_{iterations,lab}}{2\,\gamma_b^2}$$

(typically $\gamma_b \sim 10 - 60$)

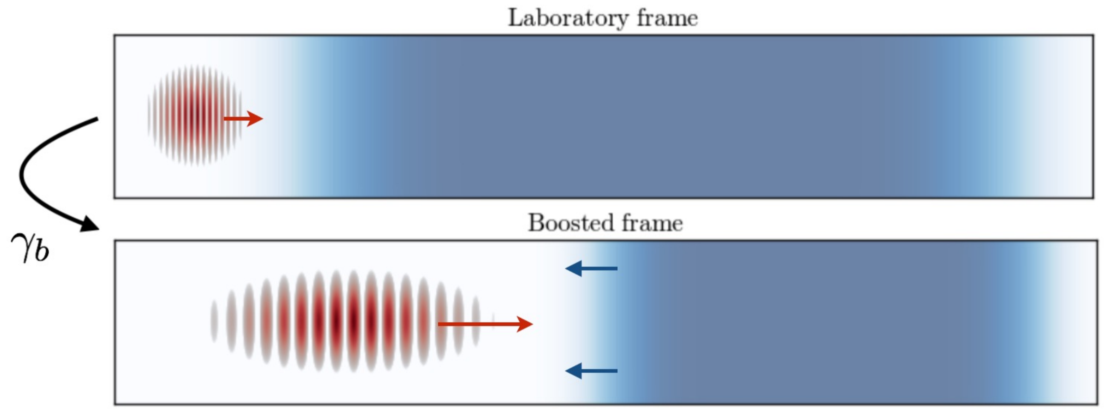

- Laser pulse ($v_{lab} \approx c$): $L_{boosted} \approx 2\gamma_b\, L_{lab}$
- Plasma ($v_{lab} \approx 0$): $L_{boosted} \approx L_{lab}\,/\gamma_b$

J.-L. Vay, "Noninvariance of Space- and Time-Scale Ranges under a Lorentz Transformation and the Implications for the Study of Relativistic Interactions", Phys. Rev. Lett. (2007)

The workflow of a lab-frame Particle-In-Cell simulation

1. Initialize the plasma and laser at t=0

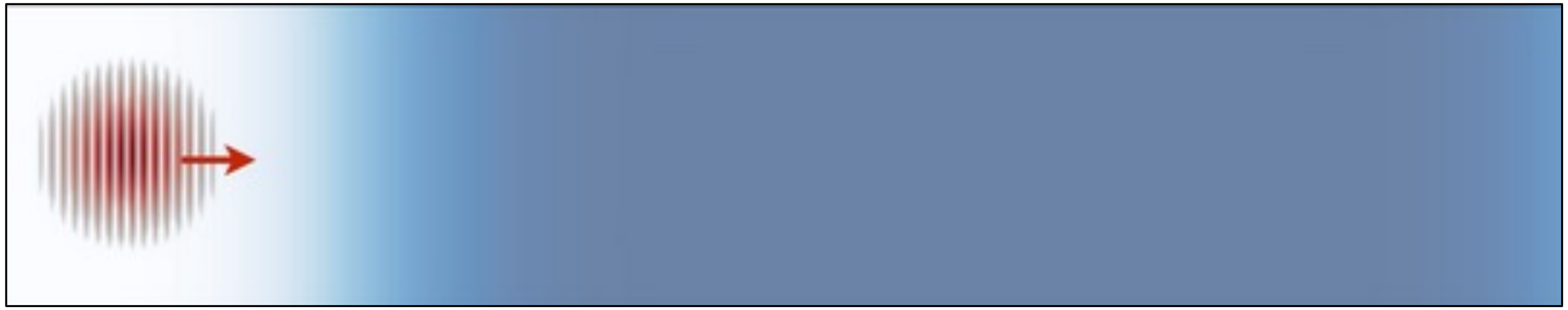

2. Repeatedly update the fields and particles, in discrete timesteps

using a discretized version of the Maxwell equations and equations of motion

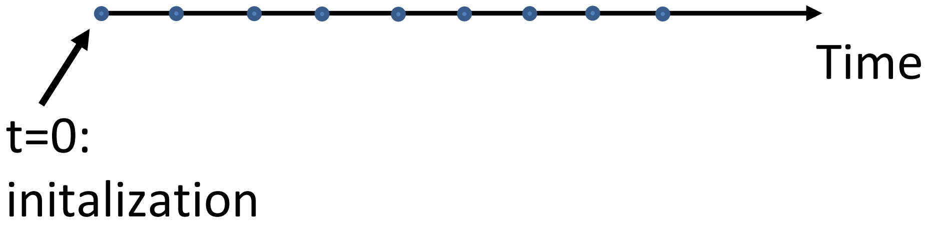

$$\partial_t \boldsymbol{B} = -\boldsymbol{\nabla} \times \boldsymbol{E}$$

$$\partial_t \boldsymbol{E} = c^2 \boldsymbol{\nabla} \times \boldsymbol{B} - \mu_0 c^2 \boldsymbol{j}$$

$$\frac{d\boldsymbol{p}}{dt} = q(\boldsymbol{E} + \boldsymbol{v} \times \boldsymbol{B})$$

$$\frac{d\boldsymbol{x}}{dt} = \boldsymbol{v} \qquad \left(\boldsymbol{p} = \frac{m\boldsymbol{v}}{\sqrt{1 - \boldsymbol{v}^2/c^2}} \right)$$

The workflow of a boosted-frame Particle-In-Cell simulation

1. Initialize the plasma and laser at t=0, in the boosted frame
(most PIC codes will automatically convert the lab-frame input parameters to the boosted frame)

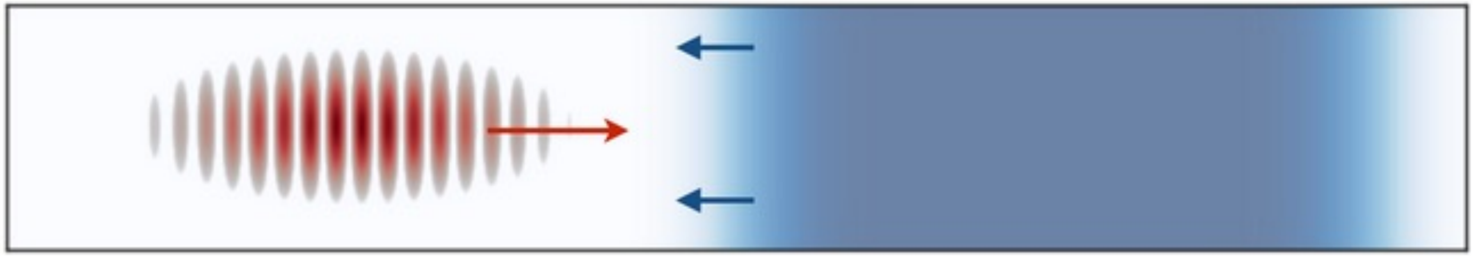

2. Repeatedly update the fields and particles, in discrete timesteps
using a discretized version of the Maxwell equations and equations of motion

Unchanged, because invariant under a Lorentz transform

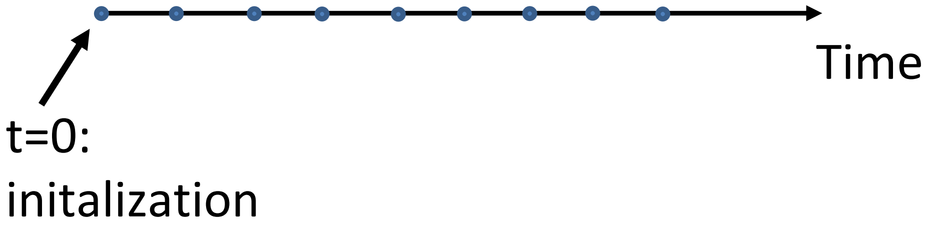

$$\partial_t \boldsymbol{B} = -\boldsymbol{\nabla} \times \boldsymbol{E}$$
$$\partial_t \boldsymbol{E} = c^2 \boldsymbol{\nabla} \times \boldsymbol{B} - \mu_0 c^2 \boldsymbol{j}$$

$$\frac{d\boldsymbol{p}}{dt} = q(\boldsymbol{E} + \boldsymbol{v} \times \boldsymbol{B})$$
$$\frac{d\boldsymbol{x}}{dt} = \boldsymbol{v} \qquad \left(\boldsymbol{p} = \frac{m\boldsymbol{v}}{\sqrt{1 - \boldsymbol{v}^2/c^2}} \right)$$

Boosted-frame simulations required specialized discretization in order to avoid numerical instabilities

With the **standard PIC discretization** (e.g. Yee solver), it turns out that relativistically-flowing plasmas are **numerically unstable**.
(Numerical Cherenkov Instability - NCI)

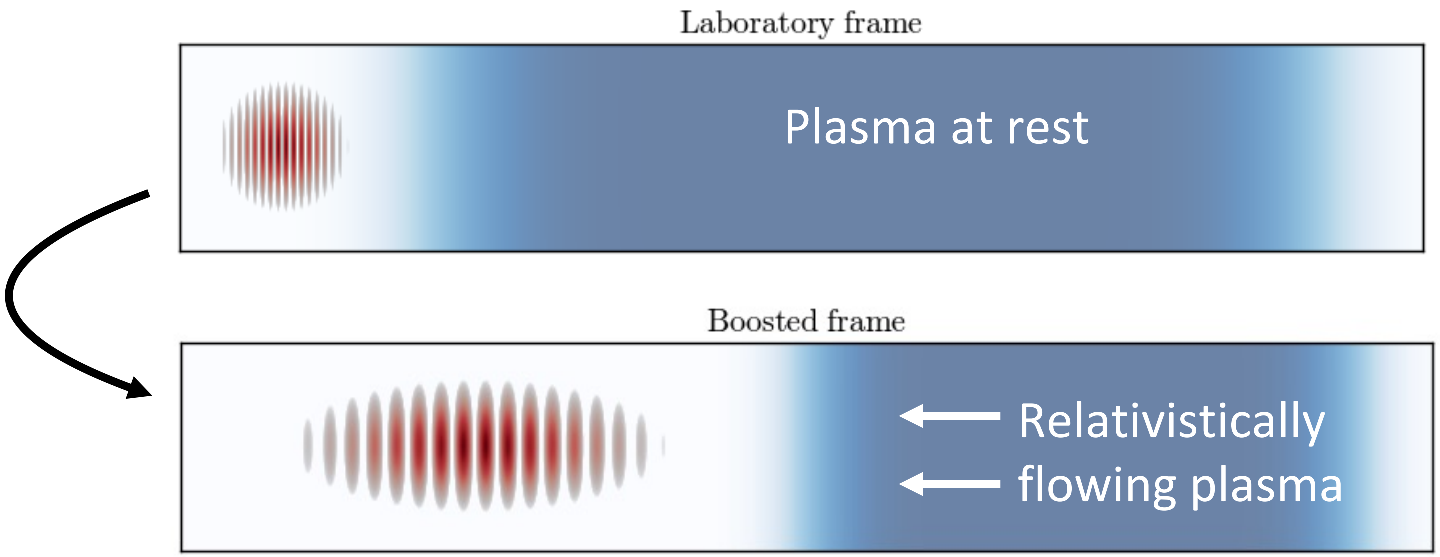

Modified discretizations have been developed in order to mitigate the NCI, e.g.

- Filtering of the gathered E&B:
  B. Godfrey et al., JCP (2014), B. Godfrey et al., CPC (2015)
- Customized Maxwell stencils:
  P. Yu et al, CPC (2015), F. Li et al, CPC (2020)
- Galilean spectral solver:
  M. Kirchen et al., PoP (2016), R. Lehe et al., PRE (2016)
- Rhombi-In-Plane solver:
  Pukhov, J. Phys.: Conf. Ser. (2019)

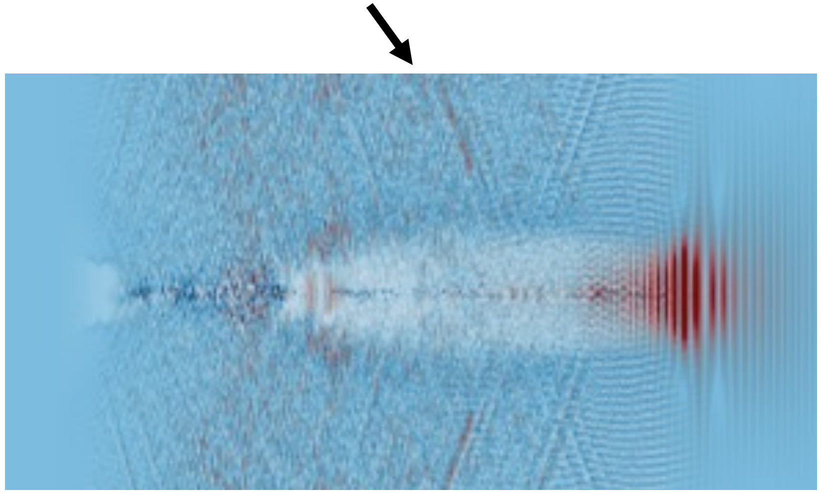

Backtransformed diagnostics allow to see the results in the lab frame.

- Looking at the **snapshots of the simulation in the boosted frame** is confusing. (As laser-plasma physicists, we are used to think in the laboratory-frame.)

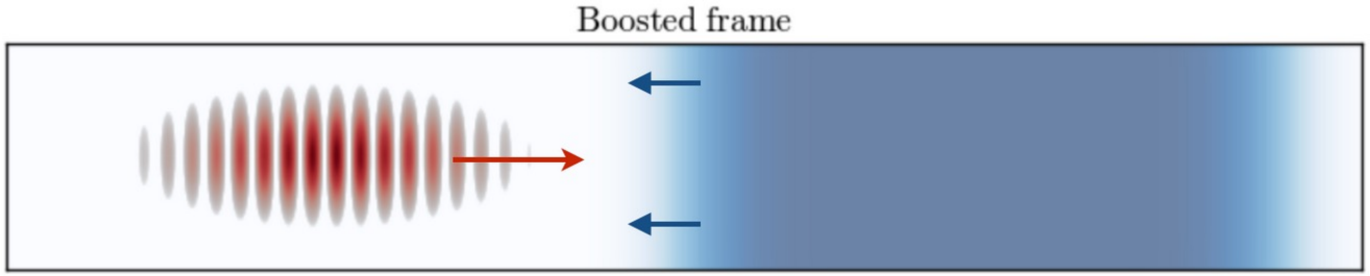

???

Backtransformed diagnostics

- Most PIC codes automatically reconstruct **snapshots in the lab frame**, while the simulation is running in the boosted-frame.

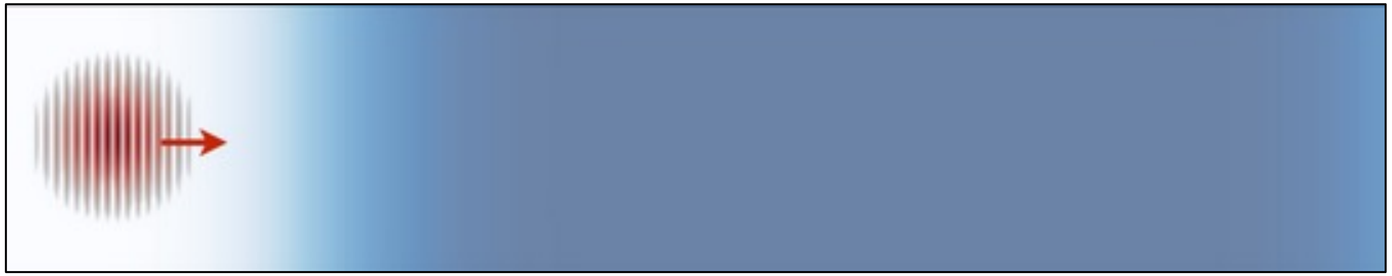

Some limitations of boosted-frame simulations

- **Backward-propagating radiation** shrinks and is **harder to resolve**.

  This e.g. prevents boosted-frame simulations of colliding pulse injection.

$$L_{boosted} = \frac{\sqrt{1-\beta_b^2}}{1-\beta_b v_{lab}/c} L_{lab}$$

Forward-propagating radiation ($v_{lab} \approx +c$):
$L_{boosted} \approx 2\gamma_b\, L_{lab}$

Backward-propagating radiation ($v_{lab} \approx -c$):
$L_{boosted} \approx \; L_{lab}/2\gamma_b$

- **Macroparticle statistics:**
  Sometimes not enough macroparticles to represent injection from the plasma.

  (Because the plasma is represented by fewer macroparticles in the boosted-frame.)

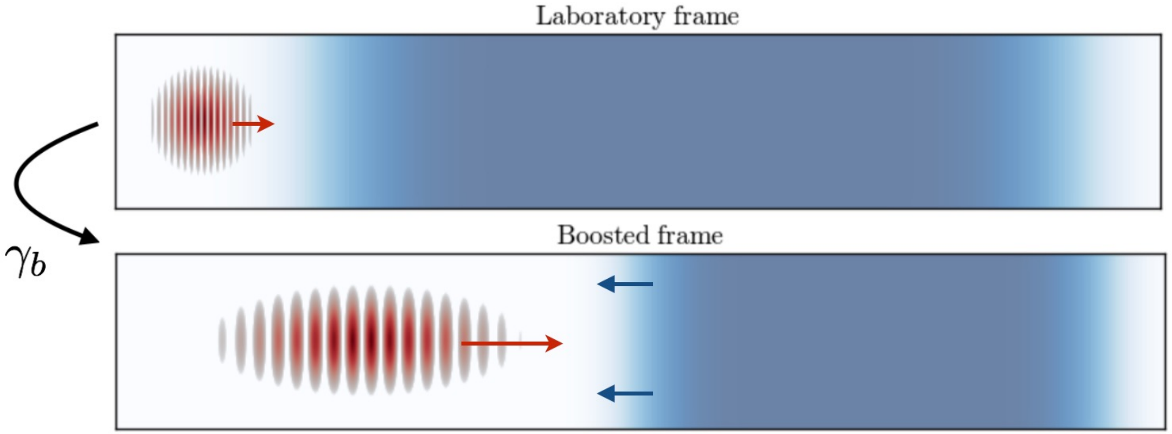

Boosted-frame technique: summary

- Runs faster by **reducing the number of PIC iterations** (by orders of magnitude)

- The simulation runs in the boosted frame,
  but the user may not notice.
  (The user provides input parameters in the lab frame.
  Simulation results are reconstructed in the lab frame.)

- Limitations: cannot model back-propagating radiation ; sometimes issues to model injection.

- Examples of codes with boosted-frame capability:
  FBPIC OSIRIS WarpX

$$N_{iterations,boosted} = \frac{N_{iterations,lab}}{2\,\gamma_b^2}$$

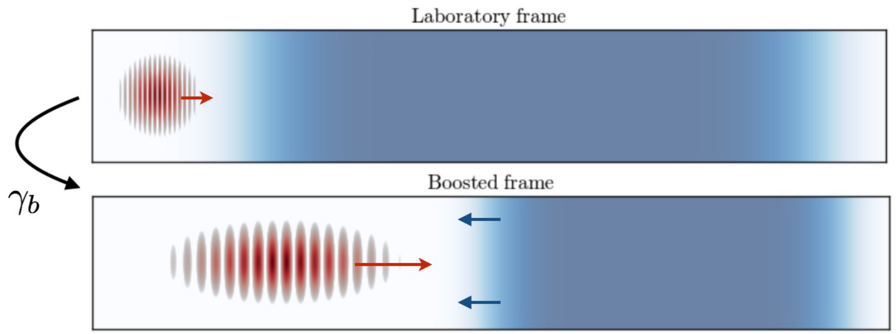

Outline

- The boosted-frame technique
- **Cylindrical geometry**
  - purely cylindrical PIC codes
  - cylindrical PIC codes with azimuthal decomposition
- Laser envelope model
- Quasi-static PIC codes

Full 3D Cartesian grids are expensive

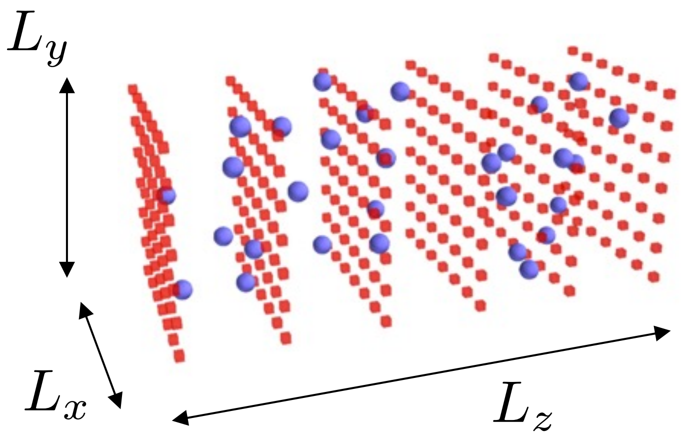

$$N_{comp} \propto \underbrace{\left(\frac{L_x}{\Delta x}\right) \times \left(\frac{L_y}{\Delta y}\right) \times \left(\frac{L_z}{\Delta z}\right)}_{\text{Number of grid points}} \times \left(\frac{T_{interaction}}{\Delta t}\right)$$

Do not use 2D Cartesian instead
(unless you really know what you are doing)

In 2D Cartesian:

- Space-charge fields do not have the right spatial structure
- Laser diffraction is not correctly captured
- Beam charge is difficult to interpret

Cartesian vs cylindrical representation

Representation in Cartesian coordinates:

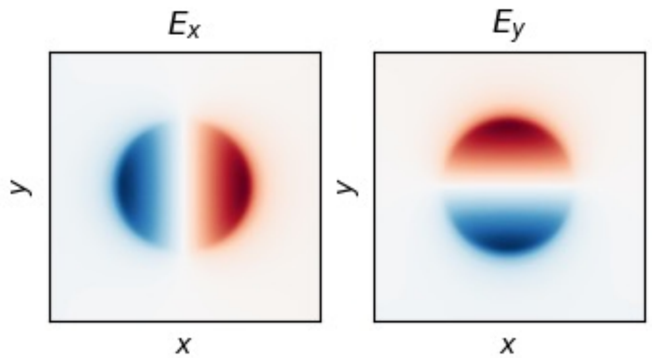

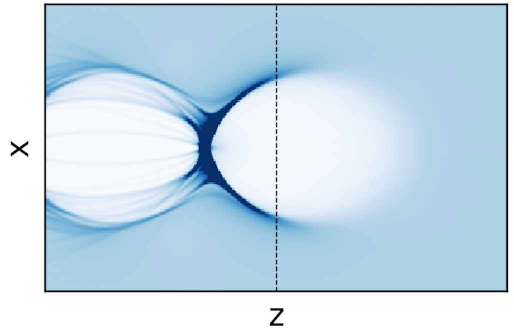

Representation in cylindrical coordinates:

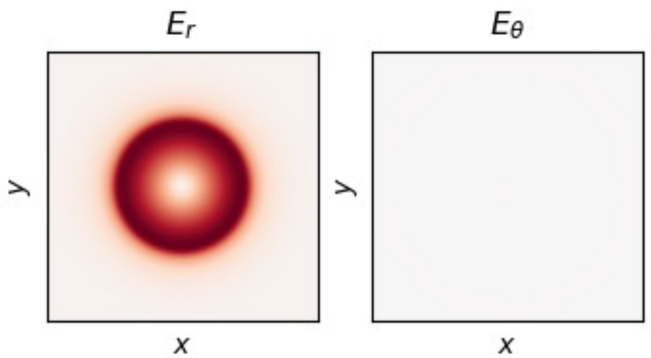

In the wakefield, fields depend on *x, y* and *z*.
We need a full 3D grid (x, y, z) to represent them.

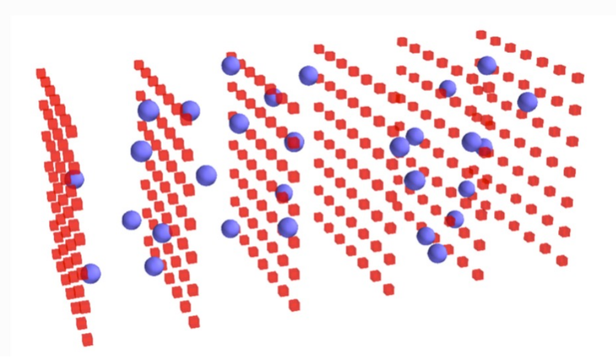

In the wakefield (for a round driver),
fields depend **only on *r* and *z*** (not on θ).
We need only a 2D grid (r, z) to represent them.

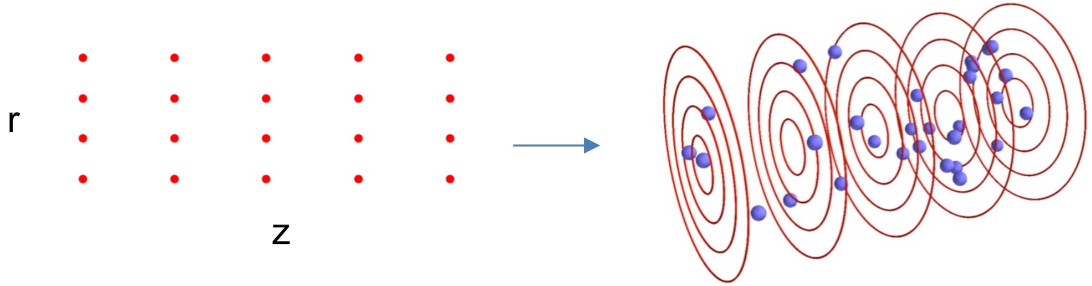

Cartesian vs cylindrical representation

Cartesian 3D PIC code:

Solve the Maxwell equations in Cartesian coordinates, e.g. for Maxwell-Faraday:

$$\partial_t B_x = -\partial_y E_z + \partial_z E_y$$

$$\partial_t B_y = -\partial_z E_x + \partial_x E_z$$

$$\partial_t B_z = -\partial_x E_y + \partial_y E_x$$

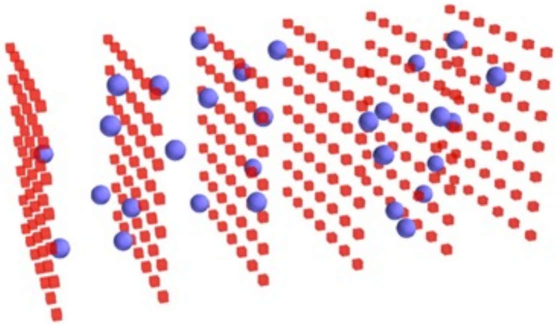

Purely cylindrical PIC codes:

Solve the Maxwell equations in cylindrical coordinates, e.g. for Maxwell-Faraday:

$$\partial_t B_r = -\frac{1}{r}\partial_\theta E_z + \partial_z E_\theta$$

$$\partial_t B_\theta = -\partial_z E_r + \partial_r E_z$$

$$\partial_t B_z = -\frac{1}{r}\partial_r r E_\theta + \frac{1}{r}\partial_\theta E_r$$

+ assume that fields depend **only on *r* and *z***, e.g.

$$E_r(r,\theta,z) = \hat{E}_r(r,z)$$

(same equation for $E_\theta, E_z, B_r, B_\theta, B_z, j_r, j_\theta, j_z, \rho$)

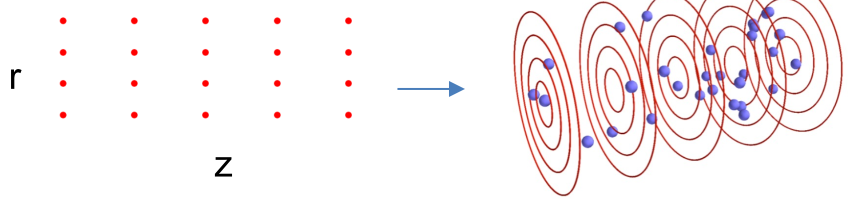

(Macroparticles usually still evolve in full 3D.)

Purely cylindrical codes are computationally much cheaper.

Cartesian 3D PIC code:

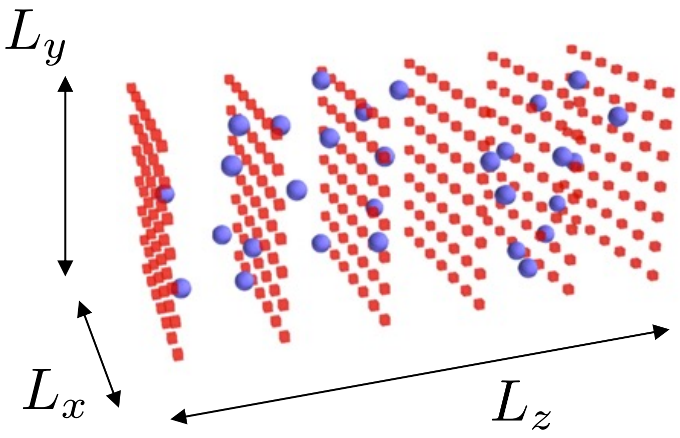

$$N_{comp} \propto \left(\frac{L_x}{\Delta x}\right) \times \left(\frac{L_y}{\Delta y}\right) \times \left(\frac{L_z}{\Delta z}\right) \quad \times \quad \left(\frac{T_{interaction}}{\Delta t}\right)$$

Purely cylindrical PIC codes:

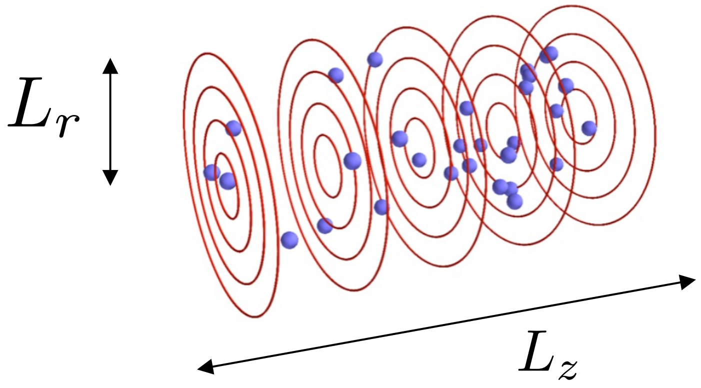

$$N_{comp} \propto \left(\frac{L_r}{\Delta r}\right) \times \left(\frac{L_z}{\Delta z}\right) \quad \times \quad \left(\frac{T_{interaction}}{\Delta t}\right)$$

Limitation of purely cylindrical PIC code: linearly polarized lasers

Purely cylindrical PIC codes can accurately capture **beam-driven acceleration** (with a round driver). However, **linearly-polarized laser pulses** are **not** properly captured:

Example: laser polarized along x
E_x and E_y do not depend on θ
(for a round intensity spot)

$$E_x(r,\theta,z) = \hat{E}_x(r,z)$$
$$E_y(r,\theta,z) = 0$$

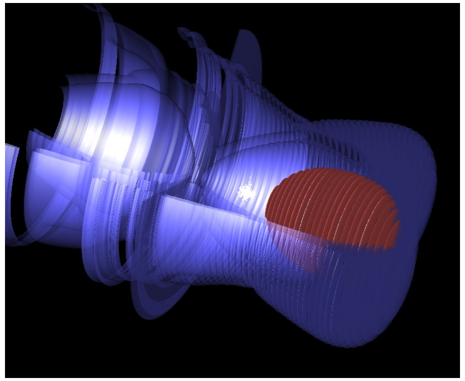

But, as a consequence,
E_r and E_θ do depend on θ

$$E_r(r,\theta,z) = \hat{E}_x(r,z)\cos(\theta)$$
$$E_\theta(r,\theta,z) = -\hat{E}_x(r,z)\sin(\theta)$$

$$\cancel{E_r(r,\theta,z) = \hat{E}_r(r,z)}$$

Going beyond purely cylindrical PIC codes: azimuthal decomposition

Represent fields as a sum of **azimuthal modes** (Fourier decomposition along θ):

$$E_r(r,\theta,z) = \mathrm{Re}\left[\sum_{m=0}^{\infty} \hat{E}_{r,m}(r,z)\, e^{-im\theta}\right]$$

+ assume that **only the first N_m modes** are important (i.e. the higher modes are negligible)

$$E_r(r,\theta,z) \approx \mathrm{Re}\left[\sum_{m=0}^{N_m-1} \hat{E}_{r,m}(r,z)\, e^{-im\theta}\right]$$

In practice, we often use:

- For beam-driven simulations: $N_m = 1$ (i.e. purely cylindrical)
- For laser-driven simulations: $N_m = 2$ or $N_m = 3$

- **Mode m=0:**
  Captures cylindrically-symmetric wakefield and space charge fields.
- **Mode m=1:**
  Captures linearly-polarized laser pulses (varies as $\cos(\theta)$, $\sin(\theta)$)
- **Modes m>1:**
  Captures additional asymmetries (varying as $\cos(m\theta)$, $\sin(m\theta)$)

A. Lifschitz et al., JCP (2009)

Going beyond purely cylindrical PIC codes: azimuthal decomposition

$$E_r(r,\theta,z) \approx \mathrm{Re}\left[\sum_{m=0}^{N_m-1} \hat{E}_{r,m}(r,z)\, e^{-im\theta}\right]$$

The modes are **not coupled** in the Maxwell equations e.g. Maxwell-Farday: for each *m*:

$$\begin{aligned}
\partial_t \hat{B}_{r,m} &= \frac{im}{r}\hat{E}_{z,m} + \partial_z \hat{E}_{\theta,m} \\
\partial_t \hat{B}_{\theta,m} &= -\partial_z \hat{E}_{r,m} + \partial_r \hat{E}_{z,m} \\
\partial_t \hat{B}_{z,m} &= -\frac{1}{r}\partial_r r \hat{E}_{\theta,m} - \frac{im}{r}\hat{E}_{r,m}
\end{aligned}$$

We can use **one r-z grid per mode**, to represent the fields and solve the Maxwell equations

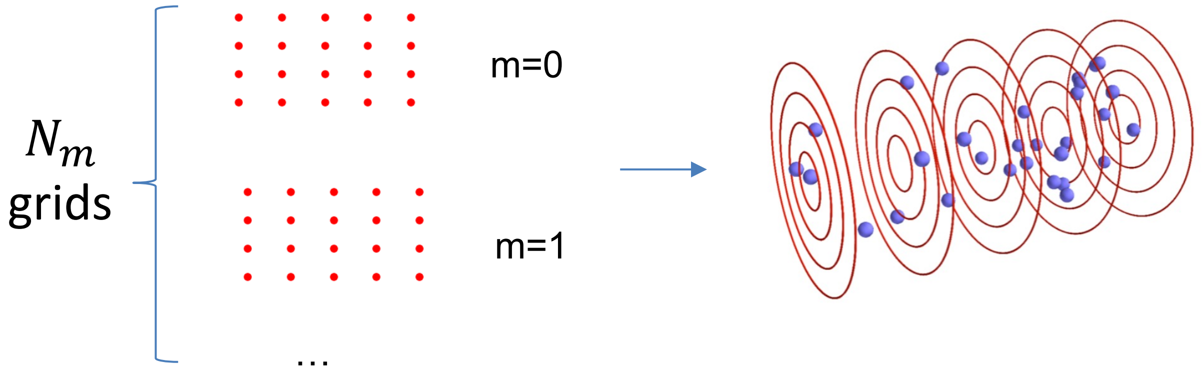

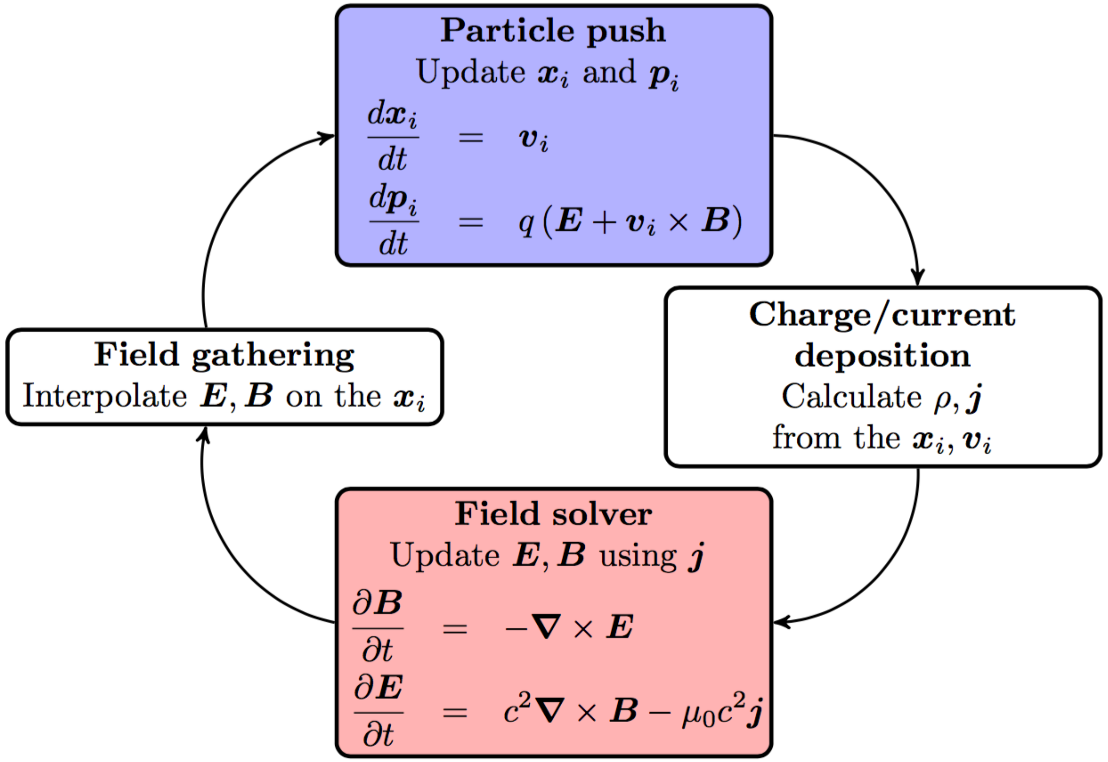

A. Lifschitz et al., JCP (2009)

Cylindrical geometry: summary

- Runs faster by reducing the **number of grid points** (one – or a few – 2D grids instead of a 3D grid)

- Can be combined with the boosted-frame technique.

- **Limitations:** with only a few azimuthal modes, some 3D effects cannot be captured, e.g.:
  - asymmetrical laser spot, pulse front tilt
  - strong misalignement between driver and beam, fully-developed hosing instability

- Examples of PIC codes with azimuthal decomposition:
  Calder Circ, FBPIC, OSIRIS, Smilei, WarpX

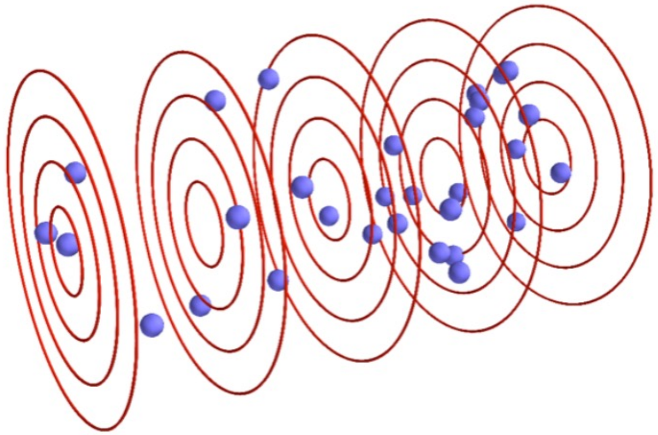

Outline

- The boosted-frame technique
- Cylindrical geometry
- **Laser envelope model**
- Quasi-static PIC codes

Full PIC simulations are expensive because they need to resolve the rapidly-varying laser field

Reminder:

- For full PIC, *E* and *B* **on the grid** represent the superposition of plasma wakefield, space-charge fields, and **laser fields**

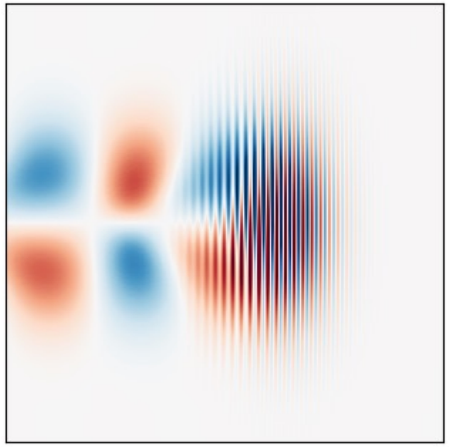

- Resolving the laser oscillations imposes high resolution in *z* and *t*

$$\Delta z \sim \frac{\lambda}{40} \qquad \Delta t \sim \frac{\Delta z}{c} \sim \frac{\lambda}{40c}$$

Maxwell's equations

$$\partial_t \boldsymbol{B} = -\boldsymbol{\nabla}\times\boldsymbol{E}$$

$$\partial_t \boldsymbol{E} = c^2\boldsymbol{\nabla}\times\boldsymbol{B} - \mu_0 c^2 \boldsymbol{j}$$

Equations of motion

$$\frac{d\,\boldsymbol{p}}{dt} = q(\boldsymbol{E} + \boldsymbol{v}\times\boldsymbol{B})$$

$$\frac{d\,\boldsymbol{x}}{dt} = \boldsymbol{v}$$

$$\boldsymbol{v} = \frac{\boldsymbol{p}}{\gamma m} \qquad \gamma = \sqrt{1 + \boldsymbol{p}^2/m^2c^2}$$

Alternative formulation: separate the slowly-varying and rapidly-varying fields

Write the fields as a superposition of **slow** and **fast** fields:

$$\boldsymbol{E} = \boldsymbol{E}_s + \boldsymbol{E}_f \qquad \boldsymbol{B} = \boldsymbol{B}_s + \boldsymbol{B}_f$$

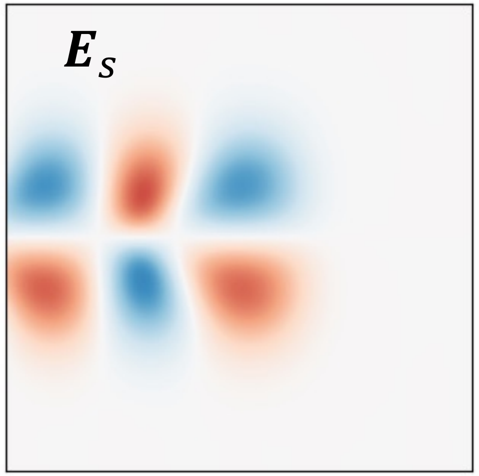

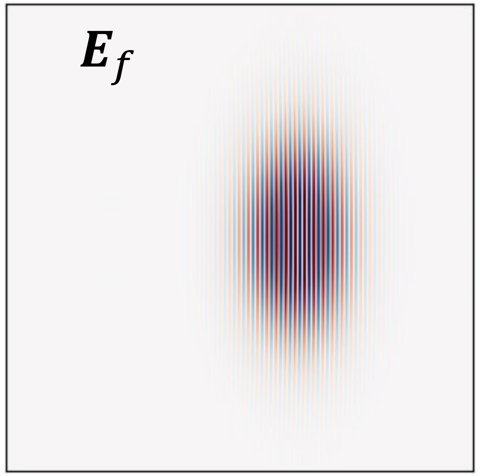

- $\boldsymbol{E}_s$, $\boldsymbol{B}_s$: slow fields (wakefield, space charge fields)

- $\boldsymbol{E}_f$, $\boldsymbol{B}_f$: fast fields (laser field)
  Often represented instead with the vector potential $\boldsymbol{A}_f$

$$\boldsymbol{E}_f = -\partial_t \boldsymbol{A}_f \qquad \boldsymbol{B}_f = \boldsymbol{\nabla}\times\boldsymbol{A}_f$$

Maxwell's equations **for the slow fields**:

$$\partial_t \boldsymbol{B}_s = -\boldsymbol{\nabla}\times\boldsymbol{E}_s$$

$$\partial_t \boldsymbol{E}_s = c^2\boldsymbol{\nabla}\times\boldsymbol{B}_s - \mu_0 c^2 \boldsymbol{j}_s$$

Equations of motion **on the slow timescale**:

$$\frac{d\,\boldsymbol{p}}{dt} = q(\boldsymbol{E}_s + \boldsymbol{v}\times\boldsymbol{B}_s) - \frac{q^2}{2\gamma m}\boldsymbol{\nabla}\langle \boldsymbol{A}_f^2\rangle$$

$$\frac{d\,\boldsymbol{x}}{dt} = \boldsymbol{v}$$

$$\boldsymbol{v} = \frac{\boldsymbol{p}}{\gamma m} \qquad \gamma = \sqrt{1 + (\boldsymbol{p}^2 + q^2\langle \boldsymbol{A}_f^2\rangle)/m^2c^2}$$

Alternative formulation: separate the slowly-varying and rapidly-varying fields

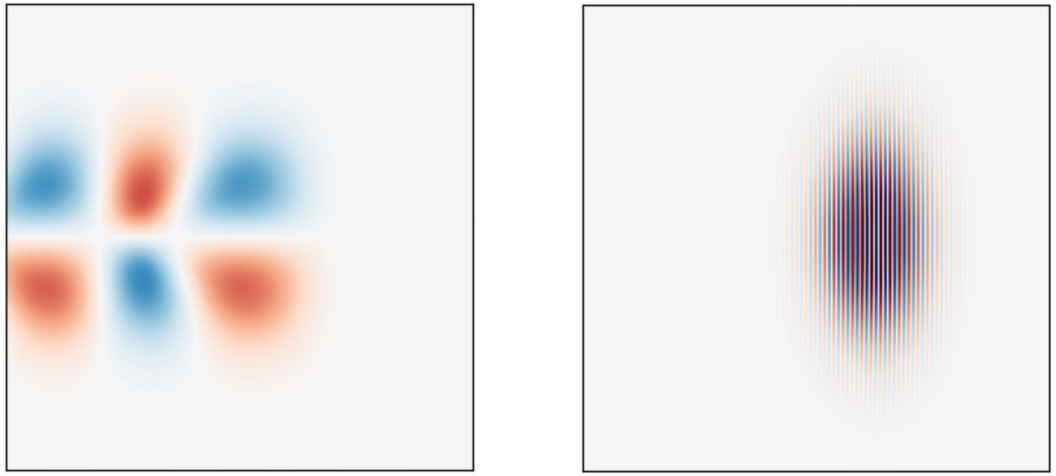

Let us drop the *s* and *f* subscripts for now on:

- $\boldsymbol{E}, \boldsymbol{B}$: slow fields (wakefield, space charge fields)
- $\boldsymbol{A}$: rapidly-oscillating laser field

Maxwell's equations **for the slow fields**:

$$\partial_t \boldsymbol{B} = -\boldsymbol{\nabla}\times\boldsymbol{E}$$

$$\partial_t \boldsymbol{E} = c^2\boldsymbol{\nabla}\times\boldsymbol{B} - \mu_0 c^2 \boldsymbol{j}$$

Equations of motion **on the slow timescale**:

$$\frac{d\,\boldsymbol{p}}{dt} = q(\boldsymbol{E} + \boldsymbol{v}\times\boldsymbol{B}) - \frac{q^2}{2\gamma m}\boldsymbol{\nabla}\langle \boldsymbol{A}^2\rangle$$

$$\frac{d\,\boldsymbol{x}}{dt} = \boldsymbol{v}$$

$$\boldsymbol{v} = \frac{\boldsymbol{p}}{\gamma m} \qquad \gamma = \sqrt{1 + (\boldsymbol{p}^2 + q^2\langle \boldsymbol{A}^2\rangle)/m^2c^2}$$

Maxwell equation for the rapidly-varying laser field and envelope approximation

Maxwell equation for the laser field *A*:

$$(\partial_t^2 - c^2\boldsymbol{\nabla}^2)\boldsymbol{A} = \boldsymbol{j}_f / \varepsilon_0 = -\frac{\chi e^2}{m_e\varepsilon_0}\boldsymbol{A} \qquad \chi = n/\gamma$$

Rapidly-varying current, due to plasma electrons oscillating in laser field

Equation for the laser envelope $\widehat{A}_{env}$:

$$(\partial_t^2 - 2i\omega_0(\partial_t + c\partial_z) - c^2\boldsymbol{\nabla}^2)\widehat{\boldsymbol{A}}_{\boldsymbol{env}} = -\frac{\chi e^2}{m_e\varepsilon_0}\widehat{\boldsymbol{A}}_{\boldsymbol{env}}$$

→ Discretization (e.g. finite-difference) on a grid that **does not need** to resolve the laser oscillations

$\chi = n/\gamma$ is computed on the grid from the macroparticles (in a similar way as $\rho, \boldsymbol{j}$ are "deposited" in full PIC)

Envelope representation:

$$\boldsymbol{A} = Re[\widehat{\boldsymbol{A}}_{\boldsymbol{env}}\, e^{\boldsymbol{i\omega_0(z/c - t)}}]$$

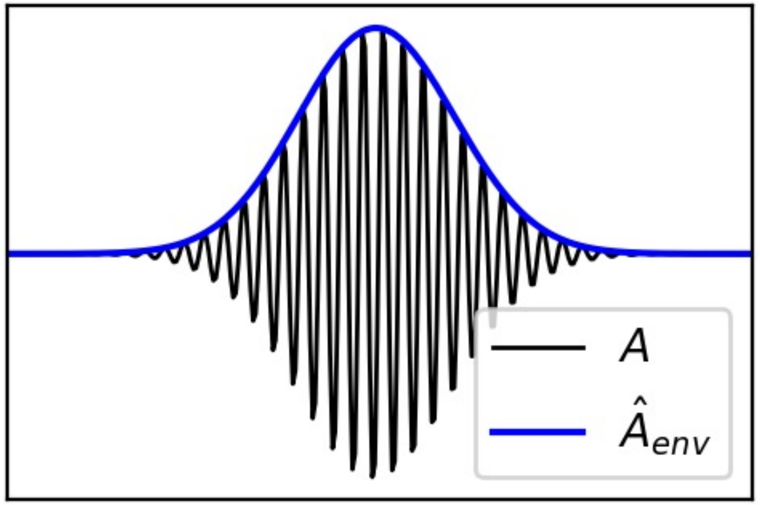

Typical lengthscale for ***A***: $\lambda_{laser} = 2\pi c/\omega_0$

Typical lengthscale for $\widehat{\boldsymbol{A}}_{\boldsymbol{env}}$: $\lambda_p \gg \lambda_{laser}$

Overview: Full PIC vs PIC with envelope model

Full PIC

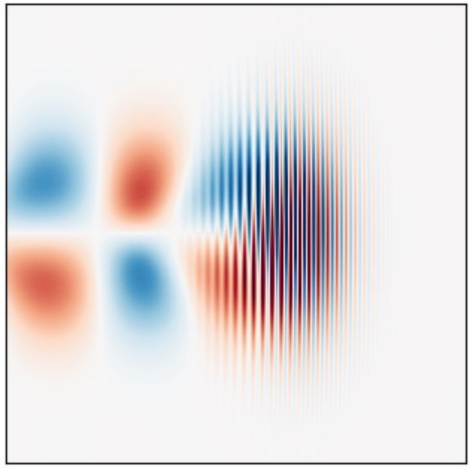

$$\partial_t \boldsymbol{B} = -\boldsymbol{\nabla}\times\boldsymbol{E}$$
$$\partial_t \boldsymbol{E} = c^2\boldsymbol{\nabla}\times\boldsymbol{B} - \mu_0 c^2 \boldsymbol{j}$$
$$\frac{d\,\boldsymbol{x}}{dt} = \boldsymbol{v}$$
$$\frac{d\,\boldsymbol{p}}{dt} = q(\boldsymbol{E} + \boldsymbol{v}\times\boldsymbol{B})$$

The grid needs to resolve the laser oscillations:

$$\Delta z \ll \lambda_{laser} \quad \Delta t \ll \lambda_{laser}/c$$

PIC with envelope model
(a.k.a. ponderomotive guiding center)

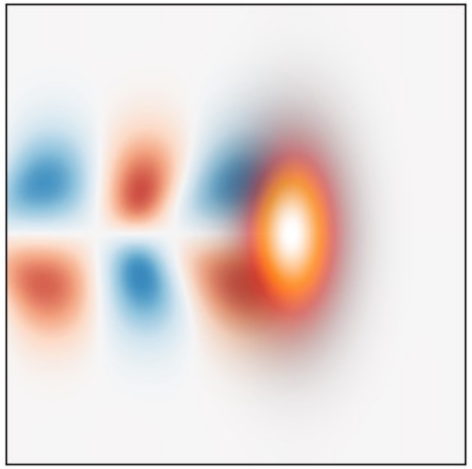

$$\partial_t \boldsymbol{B} = -\boldsymbol{\nabla}\times\boldsymbol{E}$$
$$\partial_t \boldsymbol{E} = c^2\boldsymbol{\nabla}\times\boldsymbol{B} - \mu_0 c^2 \boldsymbol{j}$$
$$\frac{d\,\boldsymbol{x}}{dt} = \boldsymbol{v}$$
$$\frac{d\,\boldsymbol{p}}{dt} = q(\boldsymbol{E} + \boldsymbol{v}\times\boldsymbol{B}) - \frac{q^2}{4\gamma m}\boldsymbol{\nabla}\left|\widehat{\boldsymbol{A}}_{\boldsymbol{env}}^2\right|$$

$$(\partial_t^2 - 2i\omega_0(\partial_t + c\partial_z) - c^2\boldsymbol{\nabla}^2)\widehat{\boldsymbol{A}}_{\boldsymbol{env}} = -\frac{\chi e^2}{m_e \varepsilon_0}\widehat{\boldsymbol{A}}_{\boldsymbol{env}}$$

The grid **does not need** to resolve the laser oscillations:

$$\Delta z \ll \lambda_p \quad \Delta t \ll \lambda_p/c$$

Laser envelope model: summary

- Runs faster by using **fewer grid points in *z*** and **fewer timesteps** (by allowing a coarser resolution in *z* and *t*)

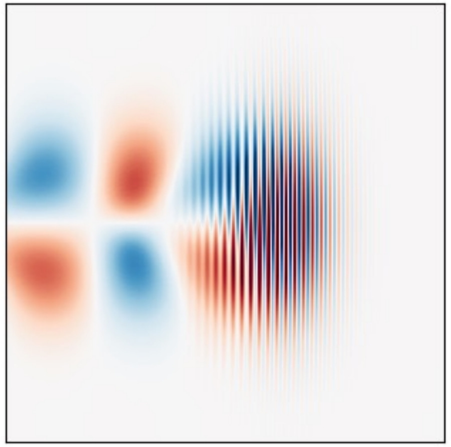

- Some limitations:
  - Other elements than the laser oscillations may actually still require high *z* and *t* resolution (e.g. sharp bubble edges, self-injection)
  - Difficulty in modeling **laser depletion** without a high resolution in z (laser wavelength changes during depletion)

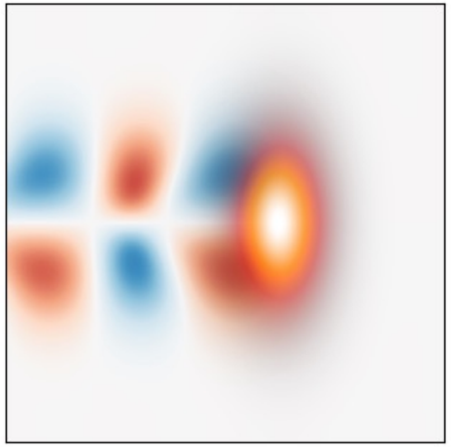

- Examples of codes with laser envelope capability:
  OSIRIS SMILEI (+ most quasistatic codes)

Outline

- The boosted-frame technique
- Cylindrical geometry
- Laser envelope model
- **Quasi-static PIC codes**

Full PIC codes do not efficiently exploit the slow beam/laser evolution

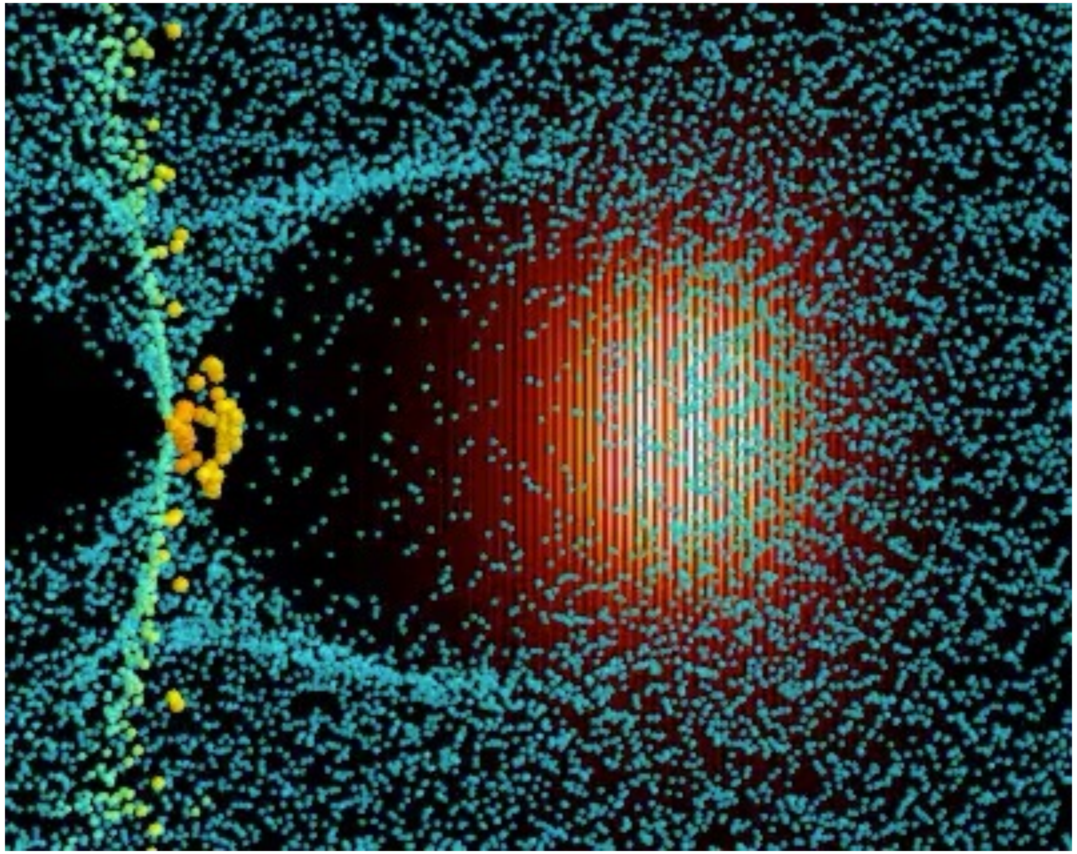

- The beam and laser evolution are **slow**:

  Beam timescale: $\tau_{beam} \sim \lambda_\beta / c$

  Laser timescale: $\tau_{laser} \sim Z_R / c$

- The overall **structure of the wakefield** also evolves on the same timescale ($\tau_{beam}, \tau_{laser}$)

- It takes a much shorter time for **plasma particles to cross the window**: $\tau_{crossing} \ll \tau_{beam}, \tau_{laser}$

  Thus, full PIC codes **effectively "recompute" the wakefield many times** over the timescale $\tau_{beam}, \tau_{laser}$ even though it does not change much.

The fields are slowly-evolving in the variables $\zeta = z - ct, \tau = t$

Fields represented as a function of z, t:

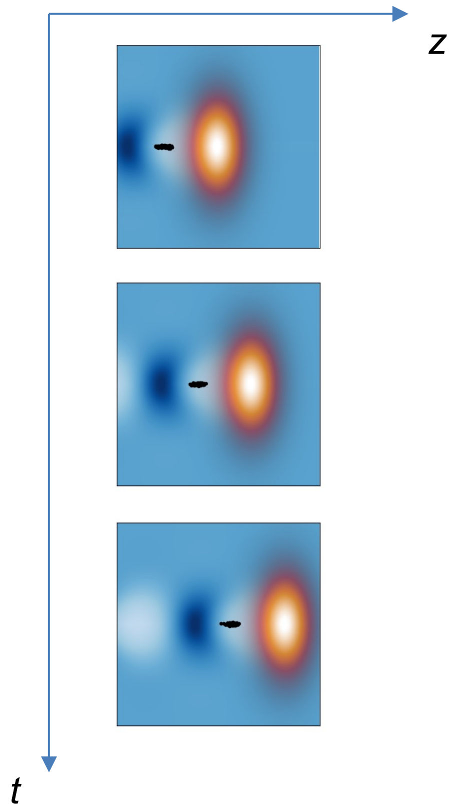

Fields vary **rapidly** as a function of:

- z (lengthscale $\sim\lambda_p$)
- t (timescale $\sim\lambda_p/c$)

(but most of the variation is simply a translation at c)

Fields represented as a function of ζ, τ:

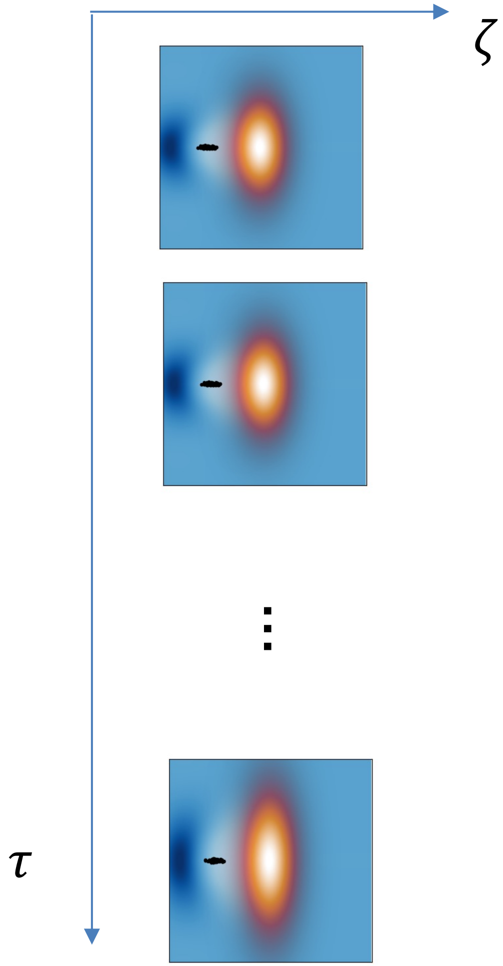

$$\zeta = z - ct$$
$$\tau = t$$

Fields still vary **rapidly** as a function of ζ (lengthscale $\sim\lambda_p$)

Fields vary **slowly** as a function of τ (timescale $\sim Z_R/c$ or $\sim\lambda_\beta/c$)

Standard PIC codes vs quasistatic PIC codes

Standard PIC code:

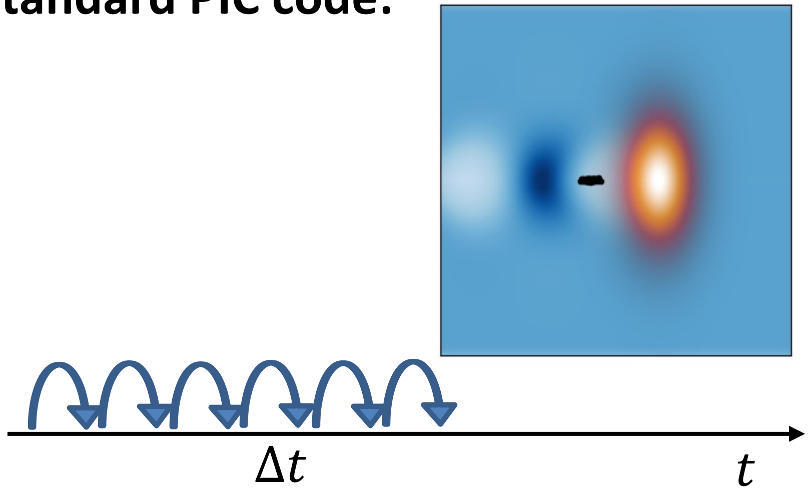

Compute the evolution of:
- beam particles
- laser (envelope)
- plasma particles

together, using the same small timestep Δt.

Quasistatic PIC code:

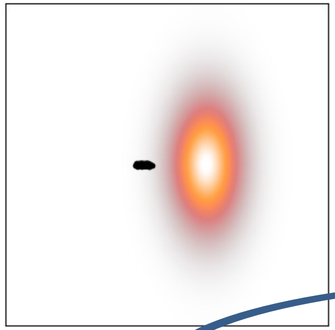

Update laser and beam, assuming that the plasma response is constant over $\Delta\tau$

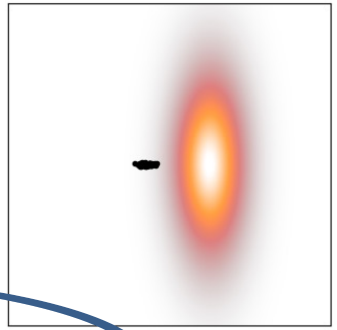

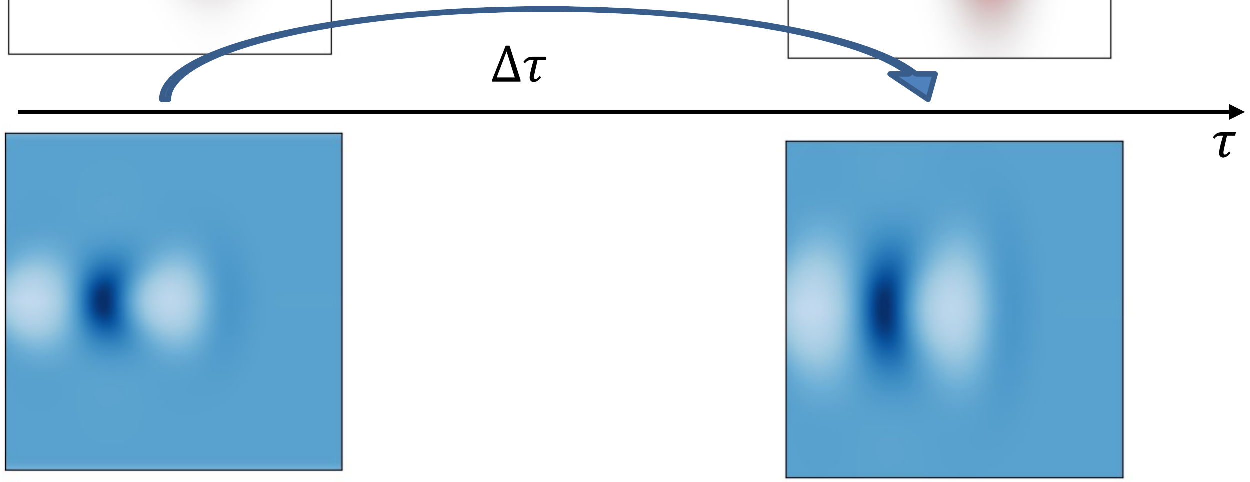

Compute **plasma response** at a fixed τ, assuming the laser and beam to be "frozen".

Equation for the (slow) evolution of the beam

For each particle of the beam:

$$\frac{d\,\boldsymbol{p}}{d\tau} = q(\boldsymbol{E} + \boldsymbol{v}\times\boldsymbol{B})$$

$$\frac{d\,\boldsymbol{x}}{d\tau} = \frac{\boldsymbol{p}}{\gamma m}$$

(unchanged compared to regular PIC)

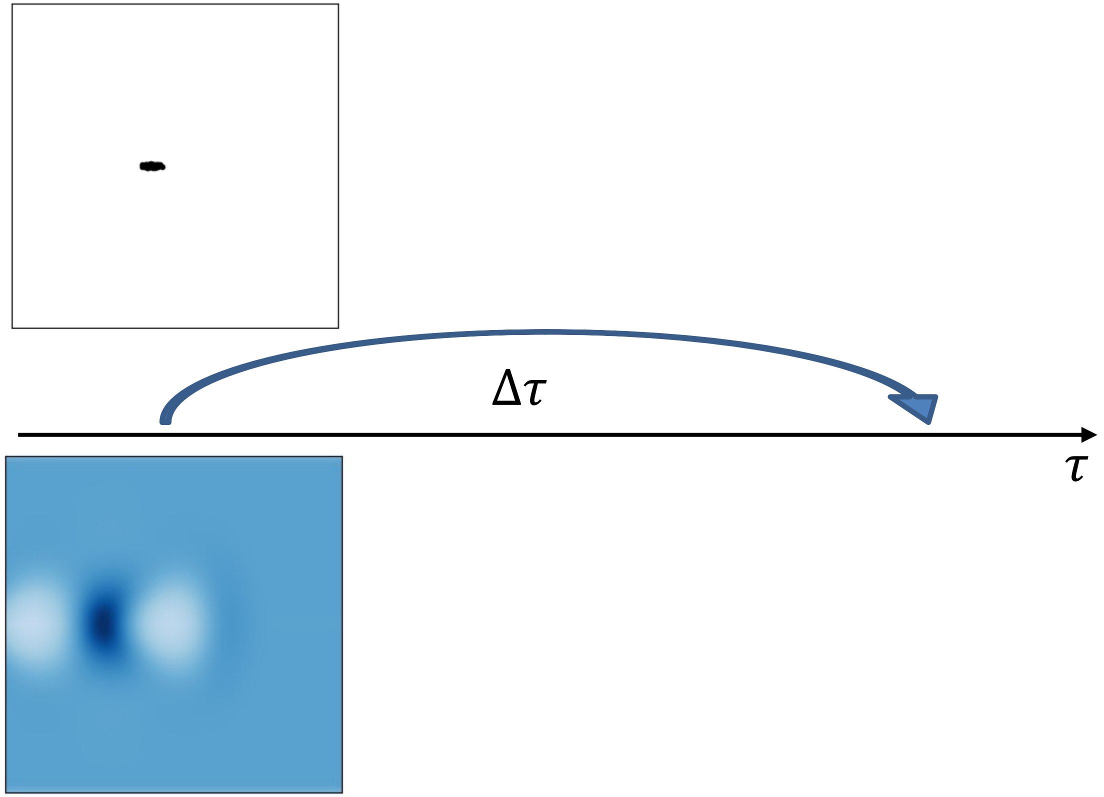

$\boldsymbol{E}, \boldsymbol{B}$: obtained from the plasma response

Equation for the (slow) evolution of the laser envelope

$$\left(\partial_t^2 - 2i\omega_0(\partial_t + c\partial_z) - c^2\boldsymbol{\nabla}^2\right)\widehat{\boldsymbol{A}}_{\boldsymbol{env}} = -\frac{\chi e^2}{m_e\varepsilon_0}\widehat{\boldsymbol{A}}_{\boldsymbol{env}}$$

Change of variable: $z, t \rightarrow \zeta, \tau$

$$\left(\partial_\tau^2 - 2i\omega_0\partial_\tau - 2c\partial_\tau\partial_\zeta - c^2\boldsymbol{\nabla}_\perp^2\right)\widehat{\boldsymbol{A}}_{\boldsymbol{env}} = -\frac{\chi e^2}{m_e\varepsilon_0}\widehat{\boldsymbol{A}}_{\boldsymbol{env}}$$

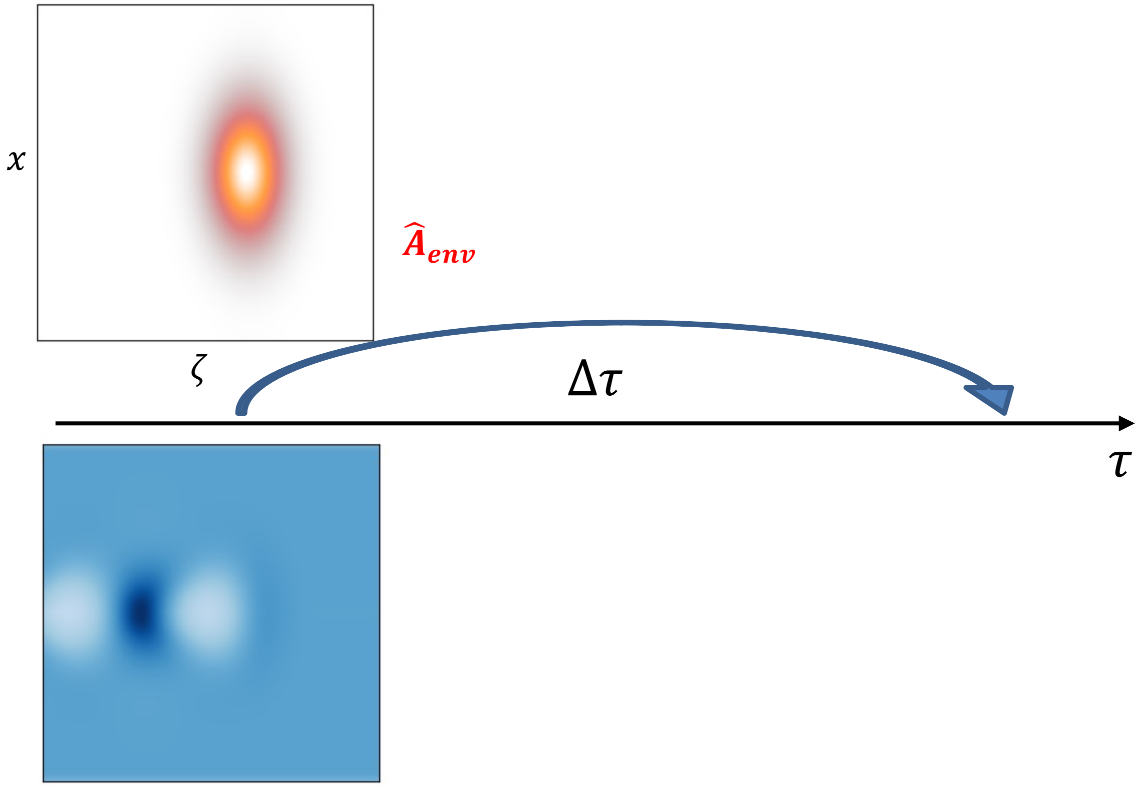

Typically integrated with an **implicit** finite-difference scheme (Crank Nicholson), that **does not have a CFL limit**. (but requires numerical inversion of the $\boldsymbol{\nabla}_\perp^2$ operator)

$\chi = n/\gamma$: obtained from the plasma response

Equations for the plasma response

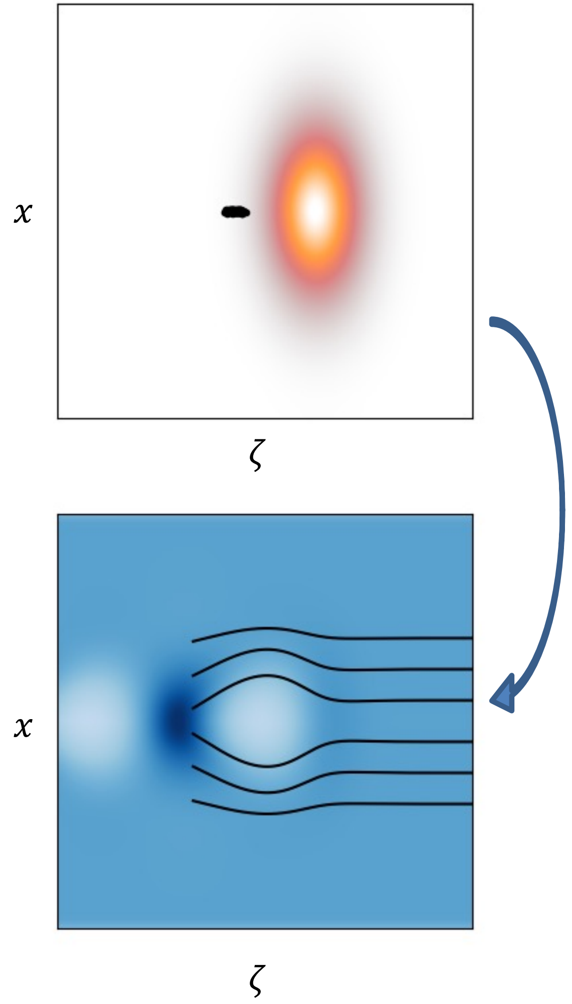

Compute **plasma response** at a fixed τ, assuming the laser and beam to be “frozen”.

In the variables ζ, τ, the plasma macroparticles “flow” through the box:

- Compute their trajectory, **parametrized by ζ** instead of t
- Compute the associated E, B in the wakefield

Equations for the plasma response

Derivation:

- change of variable $\zeta = z - ct, \tau = t$
- remove all τ dependency ($\partial_\tau = 0$)
- use conservation law for longitudinal motion

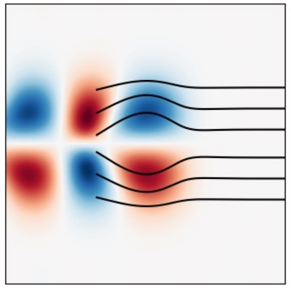

Equations for the fields on the grid:

$$\nabla_\perp^2 \psi = (j_z - \rho c)/\epsilon_0 c$$
$$\nabla_\perp^2 E_z = (\nabla_\perp \cdot \boldsymbol{j}_\perp)/\epsilon_0 c$$
$$\nabla_\perp^2 B_x = \mu_0\left(-\partial_y j_z + \partial_\zeta j_y\right)$$
$$\nabla_\perp^2 B_y = \mu_0\left(\partial_x j_z - \partial_\zeta j_x\right)$$
$$\nabla_\perp^2 B_z = \mu_0\left(\partial_y j_x - \partial_z j_y\right)$$

$$E_x - cB_y = -\partial_x \psi$$
$$E_y + cB_x = -\partial_y \psi$$

Equations of motion for the macroparticles' trajectory:

$$\frac{d\boldsymbol{x}_\perp}{d\zeta} = \frac{\boldsymbol{p}_\perp}{mc(1 + q\psi/mc^2)}$$

$$\frac{dp_x}{d\zeta} = -\frac{q\left[\gamma\left(E_x - cB_y\right) + p_y B_z\right]}{c(1 + q\psi/mc^2)} - qB_y - \frac{q^2}{4mc(1 + q\psi/mc^2)}\partial_x\left|\widehat{\boldsymbol{A}}_{\boldsymbol{env}}^2\right|$$

$$\frac{dp_y}{d\zeta} = -\frac{q\left[\gamma\left(E_y + cB_x\right) - p_x B_z\right]}{c(1 + q\psi/mc^2)} + qB_x - \frac{q^2}{4mc(1 + q\psi/mc^2)}\partial_y\left|\widehat{\boldsymbol{A}}_{\boldsymbol{env}}^2\right|$$

$$\gamma = \frac{1 + (\boldsymbol{p}_\perp^2 + q\left|\widehat{\boldsymbol{A}}_{\boldsymbol{env}}^2\right|/2)/m^2c^2 + (1 + q\psi/mc^2)^2}{2(1 + q\psi/mc^2)}$$

Algorithm for the plasma response

Fields and macroparticle positions/momenta are computed **together slice-by-slice**, from head (known initial condition: quiescent plasma) to tail

$$\frac{d\boldsymbol{x}_\perp}{d\zeta} = \frac{\boldsymbol{p}_\perp}{mc(1+q\psi/mc^2)}$$

$$\frac{dp_x}{d\zeta} = -\frac{q\left[\gamma\left(E_x - cB_y\right) + p_y B_z\right]}{c(1+q\psi/mc^2)} - qB_y - \frac{q^2}{4mc(1+q\psi/mc^2)}\partial_x\left|\widehat{\boldsymbol{A}}^2_{\boldsymbol{env}}\right|$$

$$\frac{dp_y}{d\zeta} = -\frac{q\left[\gamma\left(E_y + cB_x\right) - p_x B_z\right]}{c(1+q\psi/mc^2)} + qB_x - \frac{q^2}{4mc(1+q\psi/mc^2)}\partial_y\left|\widehat{\boldsymbol{A}}^2_{\boldsymbol{env}}\right|$$

$$\boldsymbol{\nabla}_\perp^2\psi = (j_z - \rho c)/\epsilon_0 c$$
$$\boldsymbol{\nabla}_\perp^2 E_z = (\boldsymbol{\nabla}_\perp \cdot \boldsymbol{j}_\perp)/\epsilon_0 c$$
$$\boldsymbol{\nabla}_\perp^2 B_x = \mu_0\left(-\partial_y j_z + \partial_\zeta j_y\right)$$
$$\boldsymbol{\nabla}_\perp^2 B_y = \mu_0\left(\partial_x j_z - \partial_\zeta j_x\right)$$
$$\boldsymbol{\nabla}_\perp^2 B_z = \mu_0\left(\partial_y j_x - \partial_z j_y\right)$$

$$E_x - cB_y = -\partial_x\psi$$
$$E_y + cB_x = -\partial_y\psi$$

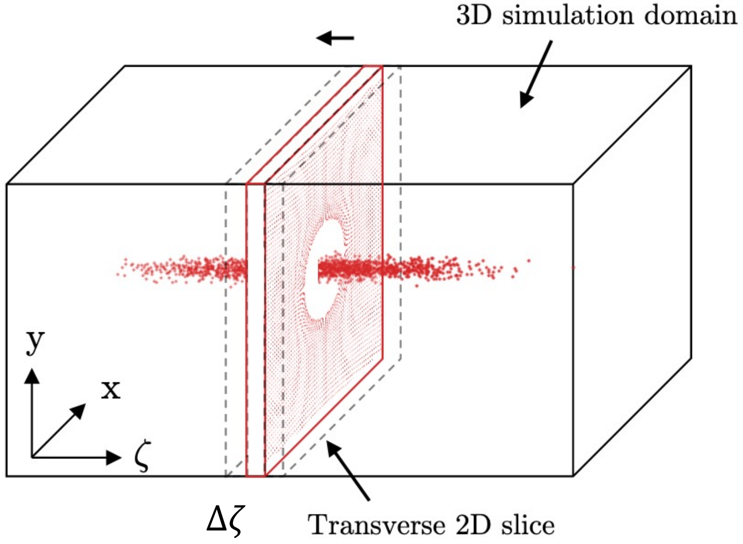

Courtesy of S. Diederichs

To go from slice ζ to slice $\zeta - \Delta\zeta$:

- Gather fields at ζ on macroparticles
- Use equation of motion to get positions/momenta at $\zeta - \Delta\zeta$
- Deposit $\boldsymbol{j}, \rho$ on the grid at $\zeta - \Delta\zeta$
- Invert $\nabla_\perp^2$ to find E, B, ψ at $\zeta - \Delta\zeta$

Quasistatic approximation: summary

- Runs faster by **reducing the number of timesteps** (by using a large $\Delta\tau$)

- Requires separating the beam/laser and plasma evolution, under the assumptions that the **wakefield structure evolves slowly**.

- Limitation: **cannot model injection from the plasma** (e.g. because of the separation between plasma and beam particles)

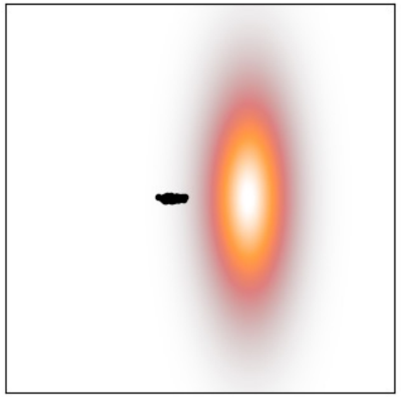

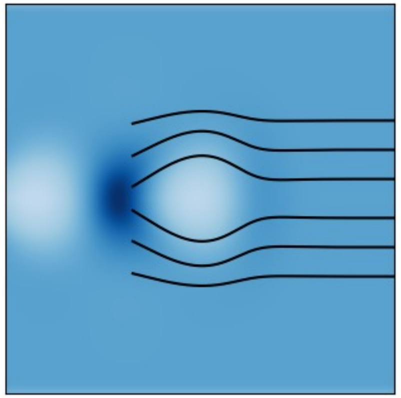

- Examples of 3D quasistatic PIC codes: HiPACE++, QuickPIC

- Some codes combine **quasistatic + cylindrical** geometry: Inf&rno, Q-PAD, Wake-T

Conclusion

- Different techniques can be used to **speed up PIC simulations**, oftentimes **by orders of magnitude**:
  - Boosted-frame
  - Cylindrical geometry
  - Laser envelope
  - Quasistatic

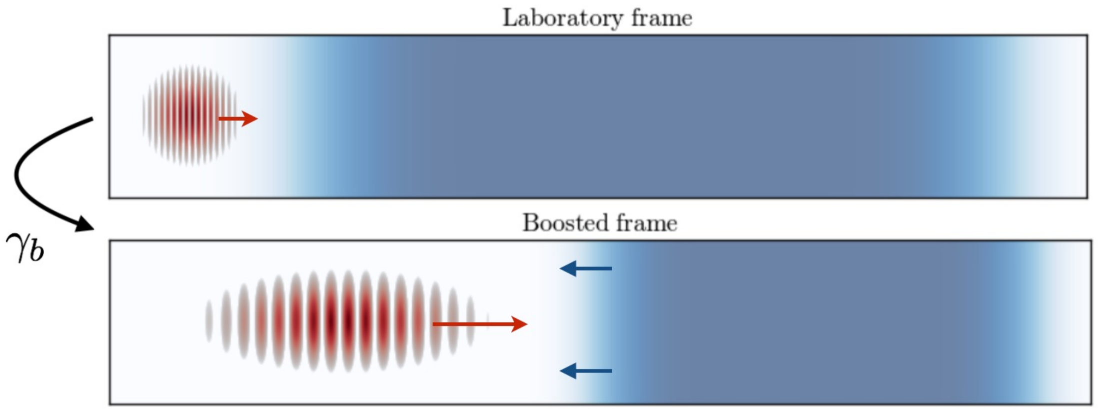

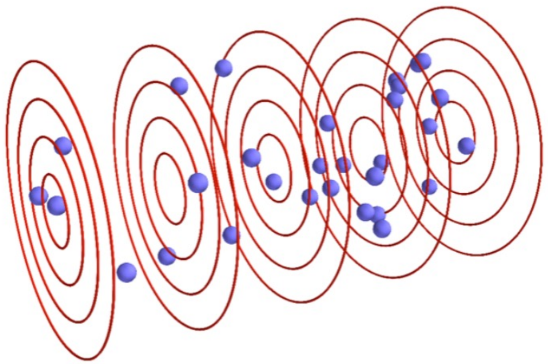

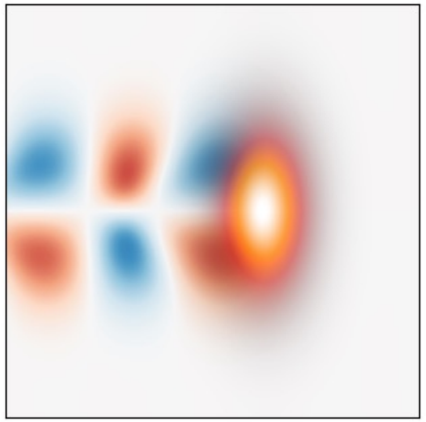

- It is nevertheless important to understand their **limitations** and in which case they are applicable.

Quick announcement: practical exercises

Monday, 6.2.	Tuesday, 7.2.	Wednesday, 8.2.	Thursday, 9.2.	Friday, 10.2.
Breakfast				
Laser-driven plasma acceleration I	Diagnostic techniques I	Laser-driven plasma acceleration II	Diagnostic techniques II	Plasma accelerator applications I
Discussion	Discussion	Discussion	Discussion	Discussion
Coffee & Tea				
Beam-driven plasma acceleration I	Modeling plasma accelerators I	Beam-driven plasma acceleration II	Modeling plasma accelerators II	Plasma accelerator applications II
Discussion	Discussion	Discussion	Discussion	Discussion
Lunch				
High-intensity lasers	Artificial intelligence and controlling acc.	Excursion	High-average power lasers	Departure
Discussion	Discussion		Discussion	
Coffee & Tea			Coffee & Tea	
Poster session I	Poster session II		Practical exercises	
Dinner				
	Special evening talk			

Please make sure you bring your **laptop**, and have an **active Google account**.

We will be using Google Colab.
(no need to install anything)

Thank you for your attention

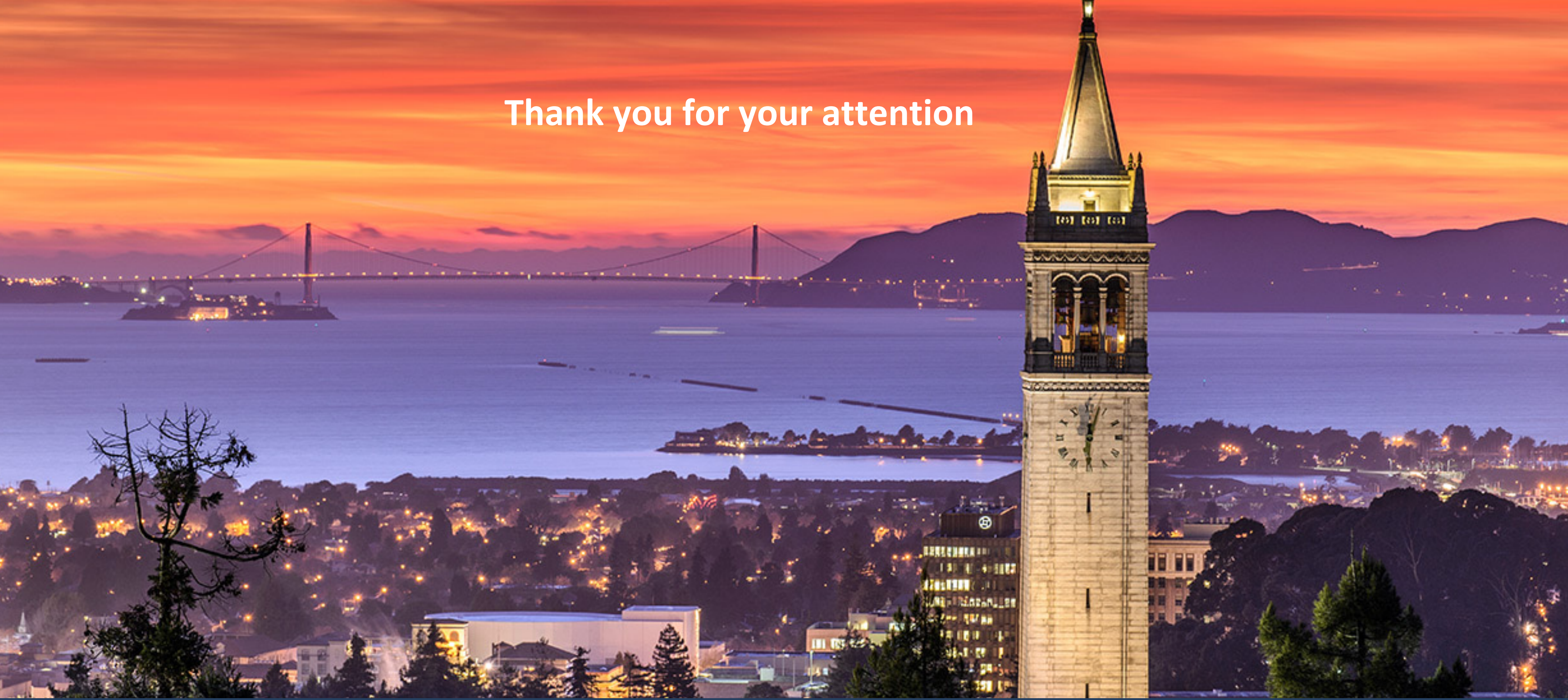

There are multiple open post-doctoral positions at the BELLA Center (theory and experiments).
If interested, please visit jobs.lbl.gov and search for “BELLA”.